Princeton Plasma Physics Laboratory

PPPL- 4953

PPPL- 4953

Non-axisymmetric Magneto-hydrodynamic Equilibrium in the Presence of Internal Magnetic Islands and External Magnetic Perturbation Coils

B.J. Tobias, M.E. Austin, I.G.J. Classen, C.W. Domier, N.C.Luhmann, Jr., and J-K Park,
C. Paz-Soldan, A.D. Turnbull, L.Yu, and the DIII-D Team

DECEMBER, 2013

PPPL PRINCETON PLASMA PHYSICS LABORATORY

Prepared for the U.S. Department of Energy under Contract DE-AC02-09CH11466.

Princeton Plasma Physics Laboratory
Report Disclaimers

Full Legal Disclaimer

Trademark Disclaimer

PPPL Report Availability

Princeton Plasma Physics Laboratory:

http://www.pppl.gov/techreports.cfm

Office of Scientific and Technical Information (OSTI):

http://www.osti.gov/bridge

Related Links:

U.S. Department of Energy

Office of Scientific and Technical Information

Fusion Links

Non-axisymmetric magneto-hydrodynamic equilibrium in the presence of internal magnetic islands and external magnetic perturbation coils

B.J. Tobias[1], M.E. Austin[2], I.G.J. Classen[3], C.W. Domier[4], N.C. Luhmann, Jr[4], J.-K. Park[1], C. Paz-Soldan[5], A.D. Turnbull[6], L. Yu[4], and the DIII-D Team

[1]*Princeton Plasma Physics Laboratory, Princeton, New Jersey, 08543-0451 USA*

[2]*Universtiy of Texas at Austin, Austin, Texas, 78712-1047, USA*

[3]*Dutch Institute for Fundamental Energy Research-DIFFER, Rijnhuizen, the Netherland*

[4]*University of California at Davis, Davis, California 95616, USA*

[5]*Oak Ridge Institute for Science Education, Oak Ridge, Tennessee 37831, USA*

[6]*General Atomics, PO Box 85608, San Diego, California 92186-5608, USA*

Abstract. Non-axisymmetric equilibria arise in DIII-D discharges that are subjected to magnetic perturbation by 3D magnetic coils. But, 3D shaping of the entire plasma, including the boundary, also occurs in the rotating fluid frame of saturated internal magnetic islands [1]. This is advantageous since internal islands and kink responses that rotate near the fluid velocity of the plasma are easily diagnosed, while static perturbations in the laboratory frame are not. The helicity of the perturbed shape is the same in both rotational frames of reference, making one mode a diagnostic proxy for the other and allowing internal modes to be used as a source of data for comparison to models typically applied to understanding the effect of static perturbations. Discrepancies with ideal magneto-hydrodynamic (MHD) equilibrium obtained by the IPEC [2] method brings attention to the treatment of plasma displacements near rational surfaces and their relationship to the accessibility of equilibrium states.

1. Introduction

Many advances in fusion science hinge upon improved understanding of 3D equilibrium. In axisymmetric configurations, such as tokamaks, we most often consider this in the context of static 3D magnetic fields that arise from engineering defects or are applied in order to improve performance [3-5]. However, we routinely diagnose interesting perturbations at the plasma boundary produced by spontaneous oscillations, particularly magnetic islands, destabilized by free energy found in the interior. For the case of 3/2 magnetic islands in DIII-D, we have observed that the plasma boundary is drawn inward, toward island O-points, and pushed outward, away from island X-points [1]. This unexpected reversal in the orientation of flux-surface-normal displacement asks us to conceive of this state as a superposition of two modes saturated in mutual force balance: a narrow island chain amplifying a global, magneto-hydrodynamic response. The latter dominates the coupling of the neoclassical tearing mode to external sensors and actuators [6, 7]. Rotating at tens of kHz and in fixed phase with the internal island, it is analyzed by signal processing techniques that have been refined for other high frequency modes [8, 9]. The 3D structure is the same as for the non-axisymmetry supported by external perturbation.

Treatment of the global non-axisymmetry associated with internal magnetic islands as an MHD response requires that it be magnetically coupled, as opposed to nonlinearly coupled through transport and the relaxation of kinetic profiles [10]. Verification of this property can be difficult because transients in low amplitude, oscillatory signal components are often obscured by noise. We overcome this by analyzing amplitude

modulation of the mode in radially localized ECE data. This technique is described in detail in Section 2.

In Section 3, MHD responses supported by internal magnetic islands are compared to those produced by the I-coil on DIII-D [11]. With respect to the poloidal mode number, or helicity of the response near the outboard midplane, we find that they are indistinguishable. Therefore, in Section 4 we compare the shared features of both cases to 3D equilibria obtained by the IPEC method. Future work discussed in the closing section of this manuscript will attempt to reconcile disagreement between experimental data and the ideal MHD model [12].

2. Identification of the magneto-hydrodynamic mode

Our approach avoids complications in directly diagnosing the plasma response to static perturbations by identifying important characteristics that are also exhibited by the global MHD response accompanying internal modes. H-mode discharges with saturated m=3, n=2 magnetic islands are chosen primarily because they have a low incidence of locked-mode disruption as compared to n=1 modes. Sheared rotation of several kHz in the core is key in the analysis, so long as it remains well below Alfvénic and acoustic velocities, ensuring that the known effects of strong rotation on mode structure are avoided [13]. Synchronous conditional averaging of ECE data over several hundred periods of island rotation has been used to produce the electron temperature fluctuations shown in Figure 1. The mode extends throughout the core and up to the edge of the plasma, but the islands themselves are never wider than 2-3 cm. Nested isothermal flux surfaces appear to be preserved elsewhere.

Inter-ELM periods provide approximately 20 ms of saturated mode behavior over which the power spectral density may be resolved to within 50 Hz. This is used to determine the quality of the oscillation by fitting the full-width at half-maximum amplitude (FWHM) of the spectral peak. As shown in Figure 2b, this fit is constant as a function of toroidal flux coordinate, revealing that drive and damping are global properties of the system. The response that extends away from the rational surface is determined to be magneto-hydrodynamic in nature by analyzing the transient response of the mode near ELM times.

The Mirnov coil signal, dominated by n=2 oscillations, is amplitude modulated at the ELM time, t_0, such that the signal due to the tearing mode behaves as $f(t) \simeq A\sin(\omega_{n2}t)\left[1 - Be^{-\alpha(t-t_0)}\right]$, where A is the n=2 amplitude, ω_{n2} the frequency, B the modulation depth at the ELM time, and α is a characteristic frequency of the recovering Mirnov coil signal amplitude. The form of AM sidebands is described by the transform relation, $A\sin(\omega_{n2}t)\cdot m(\alpha t+\beta) \Leftrightarrow iA/2\cdot\left[M(\alpha+\omega_{n2})e^{+i\beta} - M(\alpha-\omega_{n2})e^{-i\beta}\right]$, where $m(t)$ and $M(\omega)$ are the modulating function and its Fourier transform. The power spectral density of T_e fluctuations as a function of plasma radius is shown in Figure 2c. AM sidebands appear at 29.5 kHz +/- 150 Hz. The location of these sidebands and their amplitude relative to the carrier (ω_{n2} = 29.5 kHz) is constant as a function of radius, revealing that the plasma response evolves at a uniform rate and with a uniform depth of modulation.

The absolute phase of the sideband components in Fourier space, $\beta \equiv \alpha(t_d - t_0)$, is determined by the delay time of the modulation, $t_d - t_0$. FFT component phase is plotted

in Figure 2d. Data within a 99% confidence interval are shown in color for emphasis. There is no significant difference between the phase of sidebands observed at ρ=0.4 and ρ=0.9. This constrains the delay in transient behavior to an upper bound on the order of 1 μs, far too fast to be a consequence of nonlinear coupling between core and edge regions through transport or diffusive processes that would be beyond the scope of ideal MHD.

Away from the rational surface, mode structure is dominated by a MHD response. This response is compared to responses in other reference frames. In the rotating reference frame of the internal islands, force balance is established between the neoclassical mode and the ideal response. In the static, laboratory reference frame, an external current provides the force balance necessary to support an otherwise stable magneto-hydrodynamic response. The helicity of the response is the same in both cases.

3. Comparison of equilibrium in the static and rotating frames with external and internal perturbations

For a comparison of mode structure, currents in the *n*=2 I-coil array [11] on DIII-D are modulated sinusoidally with rotating phase at 10 Hz. Even parity operation, with upper and lower coils at the same phase, ensures that the equilibrium resembles the least stable helical mode. Development of this discharge is nontrivial, as I-coil modulation routinely results in a modulation of global parameters [14]. Interaction with the intrinsic error field and the rotation of the plasma response past heating and current drive sources [15] often has a variety of effects, such as the pacing of ELMs [16]. Shot #146397 has been selected because it also has a saturated 3/2 tearing mode during a window of 800 ms with variation in plasma β and ℓ_i held to less than 10%. Using as a reference a MSE constrained EFIT reconstruction of the axisymmetric equilibrium made 50 ms before the

I-coil is activated, we proceed to analyze both the slow response to external magnetic perturbation at 10 Hz and the quickly rotating response due to the 3/2 tearing mode at 29.5 kHz.

The nominally rectangular grid of local T_e measurements provided by ECE-Imaging [17] (inset boxes, Figures 3a, b) gives the variation in mode phase over approximately 0.4π radians of straight-field-line poloidal angle, θ. Data is interpolated to a full 3D reconstruction, as shown in Figures 3a and b, by assuming $d\gamma/d\theta$ is constant, where γ is the phase of the mode [9, 18]. The best fit m-number, which is not a good quantum integer [1], is presented as a function of plasma radius in Figure 3c. There is a consistency of key features between spontaneous non-axisymmetry in the rotating frame of the core tearing mode and that due to the slowly modulated I-coil perturbation. The former is diagnosed far more reliably as it is imaged over 2.5 ms (~50 periods) while global parameters are stationary. The external magnetic coils, in contrast, are modulated only 10 periods in 1 second of usable data. Subtle changes over this period ultimately lead to a locked m=2, n=1 mode disruption ~200 ms later. Repeat discharges with q_{95} between 3.3 and 3.8 produced comparable agreement between the two reference frames. In each case we image a smoothly varying, kink-like, response with m-numbers much greater than n times the local value of q.

4. A comparison to the IPEC method

The IPEC method [2] matches a spectrum of stable, ideal MHD modes obtained by energy minimization techniques in DCON [12] to a 3D field imposed by currents at an external boundary. The conditions of shot #146397 are reproduced, including a realistic model for the I-coil currents applied, and IPEC provides an ideal MHD solution for the n=2 response. This result is processed by a synthetic diagnostic [9] and then subjected to the same analysis that was performed on the real ECE-Imaging data. As shown in [Figure 4(a)], the m-number varies stepwise with radius. Near rational surfaces, poloidal mode numbers approach pitch resonant values $n*q_{\text{local}}$, and the largest m-numbers are close to $n*q_{\text{local}}+1$. This is a ubiquitous feature of potential energy minimization in ideal MHD. Large resonant displacements appear near rational surfaces and eigenfunctions transition suddenly at resonant layers. This phenomenon is demonstrated in [Figure 4(b)]. The m=3 component dominates the spectrum inside the q=1.5 surface, but there is a jump in the m=3 and m=4 components across this surface. The largest m-numbers appearing as dominant modes by our definition are determined by the spacing of rational surfaces and converge to $n*q_{\text{local}}$ for large n.

Large, sudden transitions in the radial displacement, such as those shown in [Figure 4(b)], imply an overstepping of flux surfaces that raises a number of questions and is the subject of some controversy [10]. The consequences of these discontinuities are moot, however, since they are not observed in experiment. Rather, our attention turns to principles that might be applied in order to eliminate them from our solution. The inclusion of inertia has been proposed because it penalizes large displacements with large contributions to a kinetic energy term. Applying this approach would emphasize the path

from axisymmetry to 3D equilibrium in our problem. Ignoring the accessibility of the simulated equilibrium as minimizing only the change in potential energy, δW , does, it remains that m-numbers in experiment are much larger than those in IPEC.

5. Discussion

We have demonstrated a novel method of investigating the properties of static, 3D perturbed equilibria by diagnosing the 3D shaping of the discharge induced by rotating internal magnetic islands. We verify experimentally that the rotating plasma response is a global, magneto-hydrodynamic mode. It's features are compared to externally perturbed equilibria and 3D configurations obtained in IPEC. Differences in the helicity of the modes suggest that inertia, which must be overcome in order to access 3D equilibrium, plays an important role in the prediction of ultimate structure. Without consideration of this inertia, ideal MHD allows for steps and discontinuities in radial displacement that are not observed in experiment.

As a final note, we remind the reader that experimental determination of poloidal mode number relies on a fundamental assumption about the structure of the mode with respect to straight-field-line coordinates. Namely, we require that the phase of the mode vary uniformly with the properly defined poloidal angle. Because this property is so important to the analysis, we hope to address its validity empirically through improved experimental data. This will make use of not only ECE-Imaging [17], but also the new 3D magnetic diagnostic on DIII-D [19] and advanced 2D reflectometry techniques now in development [20-22].

Acknowledgments

This work is supported in part by the US Department of Energy under DE-AC02-09CH11466, DE-FG03-97ER54415, DE-FG02-99ER54531, DE-FC02-04ER54698, and DE-FG02-95ER54309.

References

[1] B. Tobias *et al.*, Plasma Phys. Control. Fusion **55,** 095006 (2013).

[2] J.-K. Park, A. H. Boozer, and A. H. Glasser, Physics of Plasmas **14**, 052110 (2007).

[3] T. Evans *et al.*, Nuclear fusion **48**, 024002 (2008).

[4] J.-K. Park *et al.*, Physics of Plasmas **16**, 056115 (2009).

[5] A. Garofalo *et al.*, Nuclear Fusion **51**, 083018 (2011).

[6] J. Scoville, and R. La Haye, Nuclear Fusion **43**, 250 (2003).

[7] J.-K. Park *et al.*, Nuclear fusion **48**, 045006 (2008).

[8] I.G.J. Classen *et al.*, Review of Scientific Instruments **81**, 10D929 (2010).

[9] B. J. Tobias *et al.*, Review of Scientific Instruments **83**, 10E329 (2012).

[10] A. Turnbull, Nuclear Fusion **52**, 054016 (2012).

[11] G. L. Jackson, and et al., *Proc. 30th EPS Conf. on Controlled Fusion and Plasma Physics* 2003).

[12] A. Glasser, and M. Chance, in APS Meeting Abstracts (1997).

[13] M. Lanctot *et al.*, Physics of Plasmas **17**, 030701 (2010).

[14] R. Moyer *et al.*, Nuclear Fusion **52**, 123019 (2012).

[15] G. Kramer *et al.*, Plasma Physics and Controlled Fusion **55**, 025013 (2013).

[16] W. Solomon *et al.*, Bulletin of the American Physical Society **55** (2010).

[17] B. Tobias *et al.*, Review of Scientific Instruments **81**, 10D928 (2010).

[18] D. A. Spong *et al.*, Physics of Plasmas **19**, 082511 (2012).

[19] J. King *et al.*, Bulletin of the American Physical Society 8108P (2012).

[20] E. Mazzucato *et al.*, Physics of Plasmas **9**, 1955 (2002).

[21] B. Tobias *et al.*, Contributions to Plasma Physics **51**, 111 (2011).

[22] X. Ren *et al.*, Review of Scientific Instruments **83**, 10E338 (2012).

List of Figure Captions

Fig. 1. (Color online) Electron temperature perturbation as a function of radius and toroidal phase of the mode is obtained by conditional averaging over the period t = 3135-3145 ms. Radiometry is performed for a line of sight along the outboard midplane at 81° in toroidal angle. b) T_e contours (keV) in the vicinity of the island show that the region of electron temperature profile flattening extends no more than a few cm. Dashed lines represent the center positions of 2 ECE channels. Having a bandwidth of 1 GHz, radial resolution of each channel is approximately 2 cm in this region.

Fig. 2. (Color online) The modulation of n=2 magnetic fluctuation due to ELMs is observed by comparison of Mirnov and filterscope data. Time intervals used in b and c,d are labeled α and β, respectively. b) Power spectral density (PSD) as a function of radial coordinate during saturated mode behavior. Black contour denotes FWHM. c) PSD for a longer window including the effects of amplitude modulation. d) FFT phase for the same window. Color data represents a 99% confidence interval.

Fig. 3. (Color online) 2D ECE-Imaging data (inset boxes a,b) and poloidal reconstruction using fitted poloidal basis functions. a) The left box is the ECE image of an internal tearing mode. The corresponding plasma response is imaged at 19.5 kHz from t=3995 to 3997.5 ms. b) The 10 Hz response to I-coil currents averaged from t=3000 to 4000 ms. c) Poloidal mode number as a function of radius for both modes. Dashed lines indicate local values of the safety factor and harmonic multiples thereof. 5/2, 6/2, 7/2, and 8/2 surfaces are within the range diagnosed.

Fig. 4. a) IPEC mode structure subjected to poloidal mode number analysis. The staircase-like trace is the result of large, resonant displacements near rational surfaces.

b) IPEC radial displacement eigenfunctions for n=2, m=3 and m=4. The 3/2 rational surface is near Ψ=0.5.

List of Figures

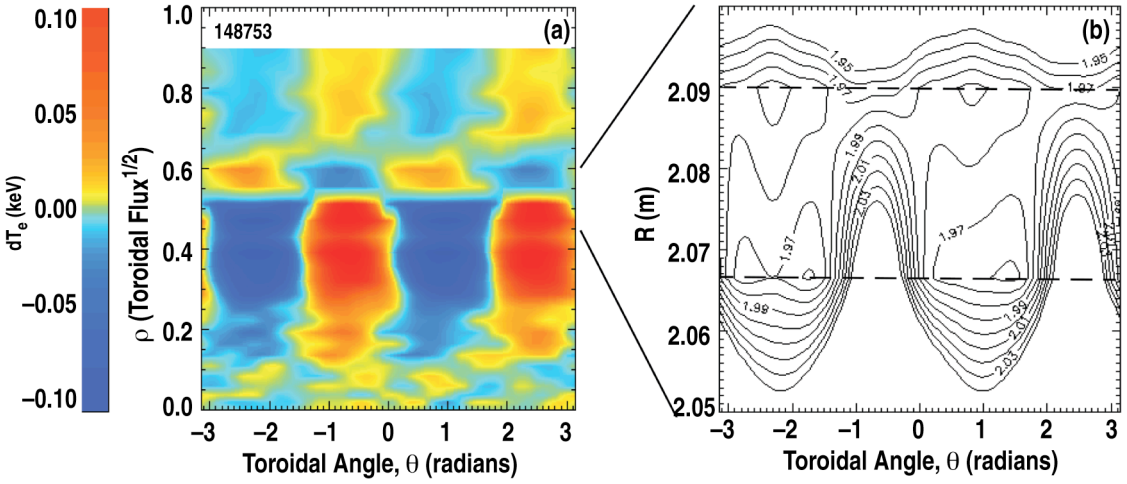

B.J. Tobias Fig. 1

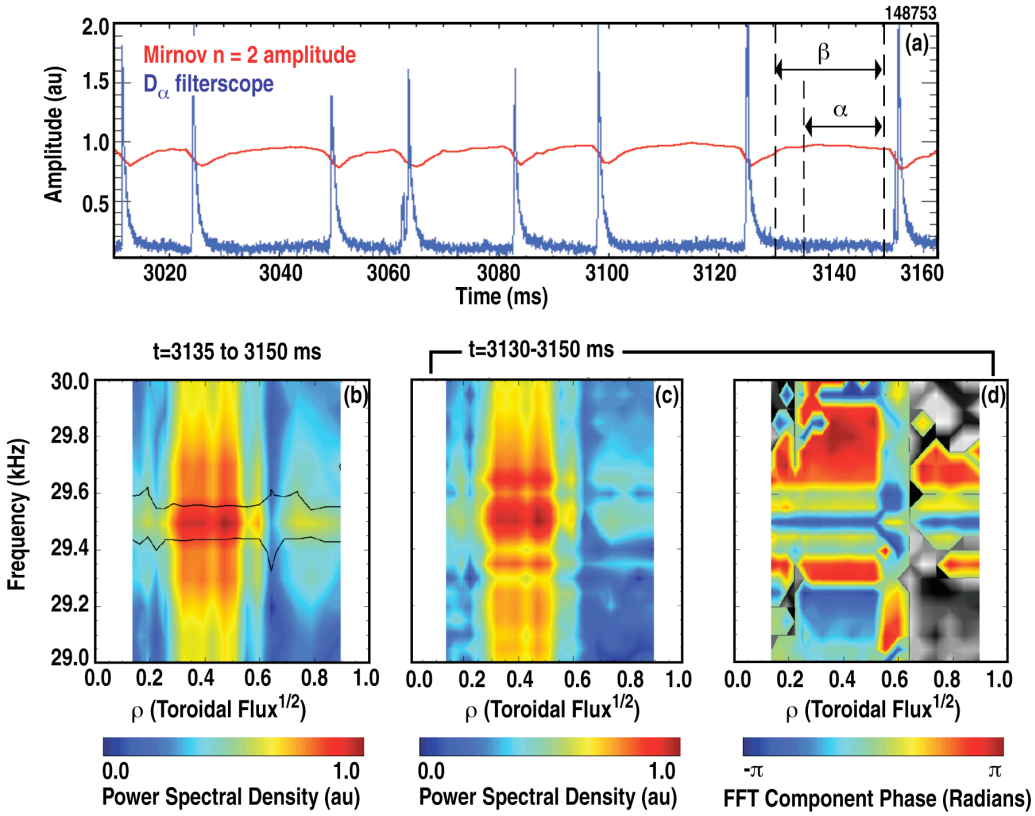

B.J. Tobias Fig. 2

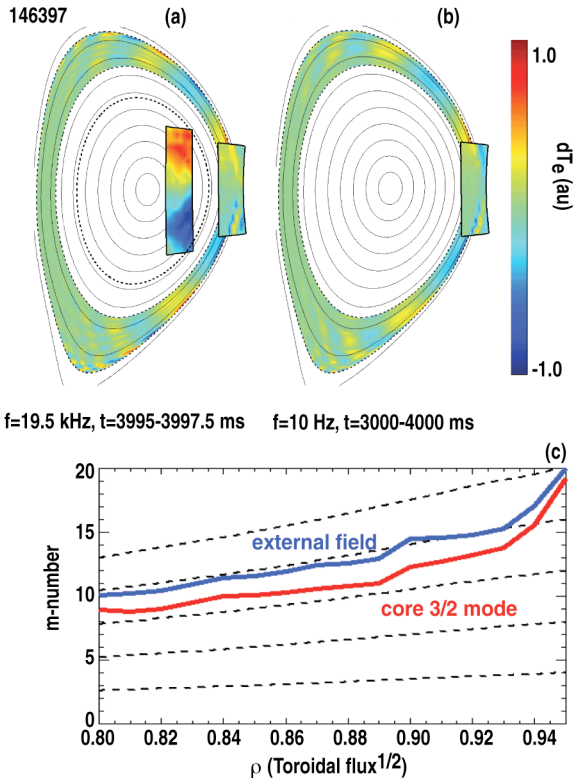

B.J. Tobias Fig. 3

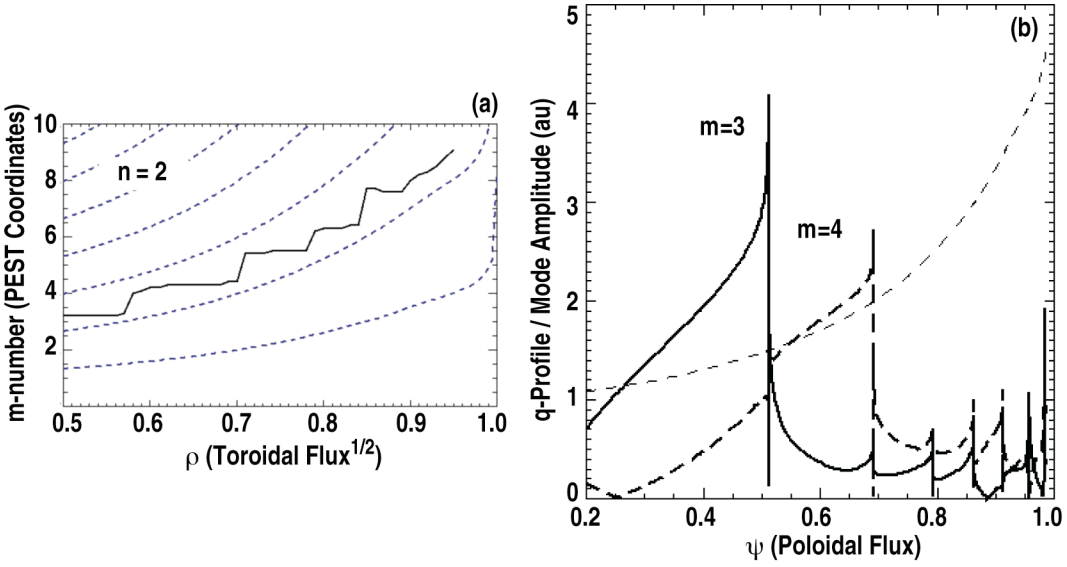

B.J. Tobias Fig. 4

The Princeton Plasma Physics Laboratory is operated
by Princeton University under contract
with the U.S. Department of Energy.

Information Services
Princeton Plasma Physics Laboratory
P.O. Box 451
Princeton, NJ 08543

Phone: 609-243-2245
Fax: 609-243-2751
e-mail: pppl_info@pppl.gov
Internet Address: http://www.pppl.gov